Dalton Transactions

PAPER

View Article Online
View Journal | View Issue

Cite this: *Dalton Trans.*, 2019, **48**, 5933

Restricted rotation of an $Fe(CO)_2(PL_3)$-subunit in [FeFe]-hydrogenase active site mimics by intramolecular ligation†

Sonja Pullen, [a,b] Somnath Maji,[a,d] Matthias Stein [c] and Sascha Ott *[a]

Received 29th December 2018,
Accepted 21st February 2019

DOI: 10.1039/c8dt05148h

rsc.li/dalton

A new series of homodinuclear iron complexes as models of the [FeFe]-hydrogenase active site was prepared and characterized. The complexes of the general formula $[Fe_2(mcbdt)(CO)_5PPh_2R]$ (mcbdt = benzene-1,2-dithiol-3-carboxylic acid) feature covalent tethers that link the mcbdt ligand with the phosphine ligands which are terminally coordinated to one of the Fe centres. The synthetic feasability of the concept is demonstrated with the preparation of three novel complexes. A detailed theoretical investigation showes that by introducing a rigid covalent link between the phosphine and the bridging dithiolate ligands, the rotation of the $Fe(CO)_2P$ unit is hindered and higher rotation barriers were calculated compared to non-linked reference complexes. The concept of restricting $Fe(L)_3$ rotation is an approach to kinetically stabilize terminal hydrides which are reactive intermediates in catalytic proton reduction cycles of the enzymes.

Introduction

[FeFe]-Hydrogenase enzymes are nature's most efficient catalysts for the reduction of protons, with turnover frequencies as high as 9000 s^{-1}.[1] The fact that the active site is held in place by the surrounding protein is crucial for this high activity, which has been revealed by analysis of the enzymes' crystal structures.[2] The binuclear active site holds a μ-bridging carbonyl ligand, and an open coordination site on one of the two iron centres. Already for a long time, it was anticipated that the reaction pathway for producing hydrogen operates *via* the formation of a terminal hydride at the iron centre that is distal to the Fe_4S_4 cluster (Fe_d). The presence of such a hydride species has first been spectroscopically implicated by H/D exchange experiments followed by FT-IR spectroscopy.[3] Final proof for the terminal hydride has only recently been established by nuclear resonance vibrational spectroscopy (NRVS), FT-IR and DFT calculations in two native proteins.[4] Biomimetic model compounds of the [FeFe]-hydrogenase active site could potentially also form terminal hydrides. DFT calculations by Hall *et al.* suggested that the first step of the catalytic cycle in such systems produces a terminal hydride as the kinetically favoured product. The terminal hydride, however, then rapidly transforms into a thermodynamically more stable bridging hydride.[5] The resulting product is rather unreactive, which is one of the major reasons why synthetic model complexes till today cannot compete with the enzyme's activity. As mentioned above, the so-called rotated structure of Fe_d with a CO bridging to the neighbouring Fe and an open coordination site is stabilized through interactions of the carbonyl and cyanide ligands at Fe_d with amino acid residues that are provided by the surrounding protein. These interactions prevent rotation of the distal $Fe(CO)_2CN$ unit after protonation, and therefore stabilize the highly reactive terminal hydride.[6] In order to design a more efficient synthetic proton reduction catalyst mimicking the active site, a similar strategy can be envisaged. This strategy to tether ligands at Fe_d models to the dithiolate linker is underexplored,[7] and different to present literature examples where a terminal hydride could be detected. With respect to the latter, three approaches have been used so far: (1) introduction of sterically demanding phosphine ligands, (2) chelating phosphine ligands or (3) increasing the basicity of the complex by using four monodentate phosphine ligands. Another family of synthetic models are mononuclear Fe-carbonyl complexes, mimicking only the Fe_d of the [FeFe]-hydrogenase active site.[8] Fig. 1 summarizes binuclear [FeFe]-hydrogenase model complexes that have been prepared in literature. The first evidence for a terminal hydride was given by Ezzaher *et al.*[9] for the complex $Fe_2(pdt)(CO)_4(\kappa\text{-dppe})$ (κ-dppe = terminal diphenylphosphin-ethylene). Treating the complex with $HBF_4{\cdot}Et_2O$ at room temperature afforded a stable

[a]*Department of Chemistry, Ångström Laboratory, Uppsala University, Box 523, 75120 Uppsala, Sweden. E-mail: sascha.ott@kemi.uu.se*
[b]*Faculty of Chemistry and Chemical Biology, TU Dortmund University, Otto Hahn Str. 6, 44227 Dortmund, Germany*
[c]*Max Planck Institute for Dynamics of Complex Technical Systems, Sandtorstraße 1, 39106 Magdeburg, Germany*
[d]*Department of Chemistry, Indian Institute of Technology Hyderabad, Kandi, Sangareddy, 502285, Telangana, India*
†Electronic supplementary information (ESI) available. See DOI: 10.1039/c8dt05148h

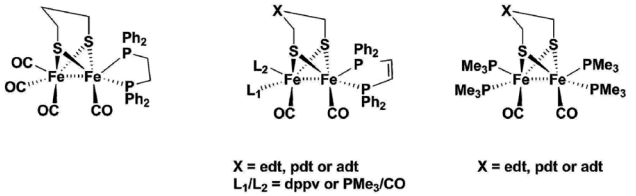

Fig. 1 Literature complexes that can form terminal hydrides.

bridging hydride which could also/even be crystallized. Low temperature NMR studies gave evidence for two terminal hydride species, one with the hydride at the substituted Fe and the other one located at the $Fe(CO)_3$ site. Following up, Adam *et al.*[10] compared a series of complexes of the types $Fe_2(pdt)(CO)_4(\mu\text{-}Ph_2P\text{-}X\text{-}PPh_2)$ (x = 2–4 CH_2) or $Fe_2(pdt)(CO)_4(\kappa\text{-}Ph_2P\text{-}X\text{-}PPh_2)$ (x = 2–4 CH_2), where the bidentate phosphine ligand was either bridging both iron atoms, or only attached to one iron centre. Bridging phosphine complexes did show that a high degree of ligand flexibility in the ligand (for n = 3 and 4) could stabilize a bridging hydride when acid was added, while the shorter dppe (x = 2) bridging ligand did not afford a detectable product. In the case where dppe or dppp were attached to only one iron atom, poorly stable terminal hydride species could be identified at low temperatures only, which rapidly transformed into the more stable bridging hydride.

Barton *et al.* worked on a series of complexes with either edt or pdt bridges and an increasing number of phosphine ligands.[11] They used a chelating bisphosphine ligand dppv (= *cis*-1,2-bis(diphenylphosphino)ethene) and PMe_3 to produce di-, tri- and tetra-substituted complexes. They found that pdt analogues showed terminal hydrides at low temperatures for the complexes with only one dppv ligand and another complex with dppv plus one PMe_3 ligand, while edt bridged complexes only showed the bridging H^-. Complexes of edt and pdt with two dppv ligands did both show terminal hydrides at low temperature and, in contrast to all earlier described models, they even exist at room temperature. The edt-analogue isomerizes within minutes, while the more stable pdt analogue has a half-life of about 10 minutes at 20 °C. They could even study the pdt analogue by cyclic voltammetry at 0 °C and show that the terminal hydride can be reduced at 200 mV milder potential than its bridging hydride isomer.[12] In summary, they concluded that isomerization of terminal hydrides can be hindered both by increasing the basicity of the diiron centre and by increasing the steric bulk of the dithiolate ligand. Barton *et al.* also suggested aza- and oxa-analogues of the pdt complexes as proton relays.[13] Carroll *et al.* picked up the suggestion and made an analogue using the adt-bridge: $Fe_2(adt)(dppv)_2(CO_2)$. With this complex, they were the first (and so far only ones) to publish a crystal structure containing a terminal hydride for the doubly protonated complex $[(term\text{-}H)Fe_2(adtH)\text{-}(CO)_2(dppv)_2]^{2+}$. In their study, they concluded that hydrogen evolution is greatly accelerated by the adt-cofactor.[14]

Finally, Zaffaroni *et al*. produced a series of tetra-PMe_3 substituted complexes with edt, pdt and adt-bridge.[15] For the edt- and pdt analogues, they propose that formation of terminal and bridging hydride are not sequential steps, but rather competing reactions. Their experiments on the edt analogue showed that at −90 °C the complex only displays the bridging hydride, while at room temperature they could observe a mixture of both the terminal and bridging hydride. For the pdt analogue, they further suggested protonation at sulfur prior to formation of the terminal hydride. Both studies used the very strong acid $H(EtO_2)_2BArF_4$. According to their study, only the adt-analogue did exclusively produce the terminal hydride even with use of weaker acids.

Schollhammer and coworkers also worked on alternative ligands for stabilizing terminal hydrides, using N-heterocyclic carbenes[16] and a mixed phosphine-carbene complex.[17] The former did not show any stable terminal hydrides even at low temperatures, while the phosphine carbene complex could hold a terminal hydride at the distal iron atom at low temperatures, which isomerized rapidly upon warming up.

All these studies show that it is indeed possible to form a terminal hydride if the complex is basic enough to be protonated rapidly. Bulky, chelating phosphine ligands further promote stabilization of the terminal hydrides, but all complexes eventually transform at room temperature into the thermodynamically more stable bridging hydride.

In the present study, we follow a new approach to hinder the rotation of the terminal ligands at one of the iron atoms. A new series of Fe_2 complexes was designed that contain terminal mono-dentate phosphine ligands covalently linked to the dithiolate bridge. This fixation of the phosphine should be able to obstruct the ligand rotation and avoid the formation of the thermodynamically more stable bridging hydride. All complexes are prepared from the hexacarbonyl precursor $[FeFe](mcbdt)(CO)_6$ **1** (mcbdt = benzene-1,2-dithiol-3-carboxylic acid). **1** contains a carboxylic acid group at the bridging benzenedithiolate ligand that can synthetically be addressed by amino-phosphine ligands to form amide bonds. Complexes **2–5** (Fig. 2) contain a tethering alkyl chain of increasing length (ethyl to pentyl) that is linked *via* an amide bond to the bridge and holds a phosphine at the end which replaces one CO ligand. Thereby, the phosphine ligands are not just coordinating to the iron centre, but they are also linked to the bridging dithiolate to obtain a more rigid structure. The hypothesis is that through this tethering effect, the rotation of the $Fe(CO)_2P$-unit will be hindered. As a result, structural rearrangements of the complex after formation of the kinetically favoured terminal hydride could potentially be prevented, or at least drastically slowed down, as compared to the situation in previous model complexes. Fig. 2(a) shows a schematic view of the [FeFe]-hydrogenase active site and its interactions with surrounding amino acid residues.[18] In Fig. 2(b), the series of model complexes with tethering ligands and a reference compound **6** with a similar set of ligands lacking the linking unit are shown. In the present study, we discuss synthesis and characterization of complexes **1**, **3**, **4** and **6**, along with a detailed theoretical investigation of all proposed compounds. In particular, we were interested in the effect of the tethering ligands on rotational energy barriers of the $Fe(CO)_2P$ unit.

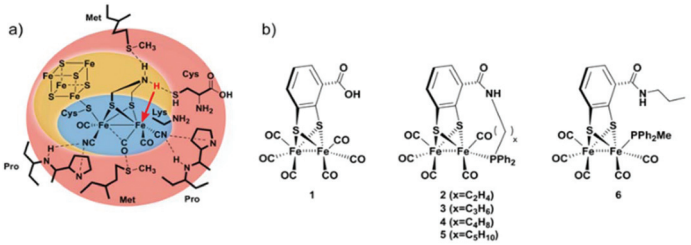

Fig. 2 (a) Coordination spheres in the [FeFe]-hydrogenase active site. Amino acid residues in the outer shell (red) stabilize the rotated geometry to form a terminal hydride. (b) Series of model complexes presented in this study. Complexes **2–5** contain an alkyl-chain tethering the bridging dithiolate ligand and a phosphine ligand.

Results and discussion

Synthesis

Synthesis of complexes **1**, **3**, **4** and **6** is described in detail in the Experimental section. A representative synthetic procedure for tethering phosphine containing complexes is outlined for the example of **3** in Fig. 3. Briefly, starting with [FeFe](mcbdt)$(CO)_6$ **1**, an amide bond is formed by the reaction between the amine functionalized phosphine ligand and the carboxylic acid. A suitable coupling reagent for this transformation was found to be PyBop (benzotriazol-1-yl-oxytripyrrolidinophosphonium hexafluoro-phosphate). Continuous stirring for about five hours at room temperature leads to substitution of one carbonyl ligand at the iron centre. Reference compound **6** was synthesized in two steps, starting with the amide coupling of propylamine to the carboxylic acid and subsequent ligand exchange with PPh_2Me. In order to selectively introduce only one $P(Ph)_2Me$ ligand, one equivalent Me_3NO as decarbonylation reagent was added to the reaction. All complexes where characterized by IR, ^{31}P-NMR and HR-MS in case of **3** and **4** (see ESI† and Experimental details).

IR spectroscopy

Coordination of the tethered phosphine ligands is clearly indicated in the IR spectra by a shift of the carbonyl stretching frequencies by about 30 cm^{-1} towards lower wavenumbers compared to that of the hexacarbonyl starting material **1** (Fig. 4 and Table 1). Spectra of **3**, **4** and **6** are largely identical, suggesting that neither the presence of the tether, nor the presence of different tethers has a profound impact on the electronic properties of the Fe sites.

As expected, also potentially different rotational isomers that arise from preferred apical or basal coordination modes

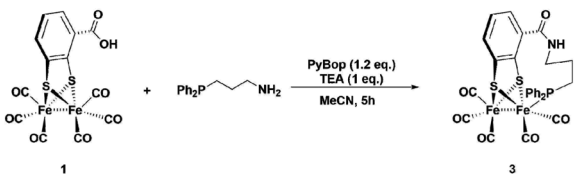

Fig. 3 One-pot synthesis of the propyl-tethered complex **3**. Complexes **4** was prepared in a similar fashion.

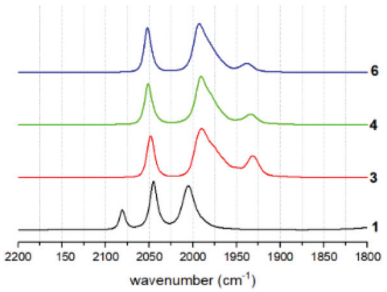

Fig. 4 IR spectra of tethered complexes **3** and **4**, reference complex **6** and hexacarbonyl precursor **1**.

Table 1 ν_{CO} stretching frequencies of synthesized complexes **1–6** compared to calculated structures

Compound	ν_{CO} exp. cm^{-1}	ν_{CO} calc. cm^{-1}
1	2081, 2045, 2005	2061, 2030, 1998
3	2048, 1989 (b), 1931	2040, 1988, 1929
4	2051, 1992 (b), 1934	2037, 1989, 1935
6	2052, 1993, 1938	2041, 1984, 1943

in the different compounds cannot be clearly identified by the indistinguishable IR spectra. This behaviour is identical to all other mono-phosphine complexes of this type in the literature.[19] Presumably, the rotational isomers rapidly interconvert, as supported by the fact that only one resonance is observed in the ^{31}P solution NMR spectra of the compounds. Calculations of carbonyl stretching frequencies clearly show that the experimental spectra are a 1 : 1 superposition of terminal and apical ligand species (see below).

DFT calculations

Structural optimizations were conducted with the BP86 functional and a def2-TZVP basis set for all rotational isomers in order to identify the thermodynamically most favoured structures. This method has been shown to give accurate data for the precursor complex [FeFe](mcbdt)$(CO)_6$ **1** compared with the crystal structure (see Table S5 in ESI†). All calculated structures were true minima as indicated by vibrational frequency analysis (see Fig. 5 for comparison between experimental and calculated spectra). Additional

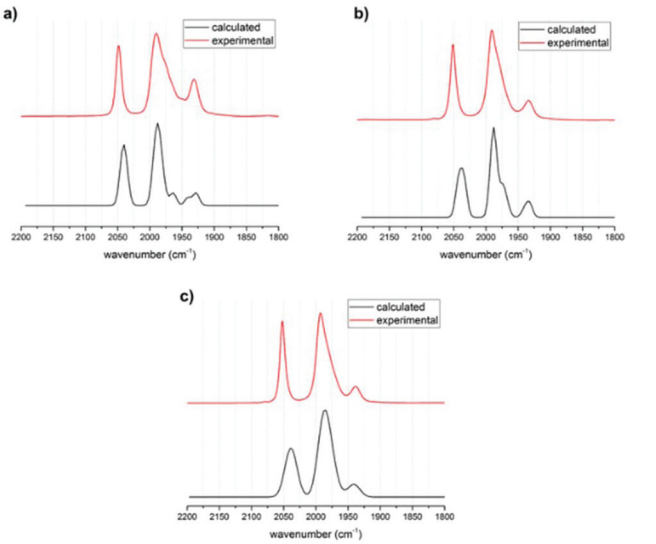

Fig. 5 Calculated (black) and experimental (red) IR spectra of (a) **3**, (b) **4** and (c) **6**. The calculated spectra are 1 : 1 mixtures of the spectra obtained for the apical and basal isomers with BP-86 without use of scaling factor.

single point energy calculations using the hybdrid B3LYP, the double-hybrid PWPB95 functional and local coupled-cluster DLPNO-CCSD(T) were performed in order to systematically increase the accuracy of calculated energy barriers B3LYP, PWPB95 and DLPNO-CCSD(T).

First, the structures of complexes **3** and **4** as well as that of the reference complex **6** were optimized. Vibrational frequency analysis was performed for all three structures and the results are in good agreement with experimental data (Table 1). No scaling factor was used. The calculated IR spectra for the phosphine in apical *versus* basal position were very similar in shift, but there was an additional peak found for the basal structures (see Fig. 5). In the experimentally obtained spectrum, this peak in the centre of the spectrum around 1990 cm^{-1} is very broad and has a shoulder. Comparing the calculated spectra with experimental suggests that for all structures the apical and the basal isomers both are present in equilibrium. The visualized calculated spectra in Fig. 5 are a superposition of the calculated spectra of the apical and basal isomers in a ratio of 1 : 1. When the structures were calculated with PMe_2 instead of PPh_2, the shape and frequency of calculated IR absorption bands do not change significantly (ESI Fig. S6†). Since the PMe_2-substituted complexes resemble the structure PPh_2-substituted complexes very well, the following calculations concentrated on PMe_2-substituted isomers. This computational modification is indicated by a "Me" as index to the compound number, *e.g.* ($\mathbf{3}^{\mathbf{Me}}$).

Computational design of tethering. In addition to the synthetically derived complexes two further model compounds with ethyl- (**2**) and pentyl- (**5**) chains were investigated computationally. The full series of model structures with different chain-lengths (CH_2 = 2–5), phosphine ligands and substitution positions (apical *vs.* basal) was investigated in order to gain a systematic insight into the influence of the tethering ligand carbon chain length and to identify the thermodynamically most favoured products (see Table 2). Table S2† gives an overview over the geometry optimized lowest energy structures for all these complexes. When the alkyl chain contains 3–5 carbon atoms, both the apical and the basal isomers are feasible. An ethyl chain is too short to connect a basal phosphine ligand with the bridging bdt and only the apical form is accessible. A structure for the apical isomer of **2** is included in the ESI.†

Table 2 Calculated energy differences between the apical and basal structures of complexes $\mathbf{2}^{\mathbf{Me}}$–$\mathbf{6}^{\mathbf{Me}}$ ΔE = E(apical) − E(basal) in kJ mol^{-1}. A negative energy indicates the preference of the apical form

	BP86	B3LYP	PWPB95	DLPNO-CCSD(T)
$\mathbf{2}^{\mathbf{Me}}$	n.a.[a]	n.a.[a]	n.a.[a]	n.a.[a]
$\mathbf{3}^{\mathbf{Me}}$	−5.6	−12.8	−3.2	−14.1
$\mathbf{4}^{\mathbf{Me}}$	+11.0	+8.2	+9.1	+3.9
$\mathbf{5}^{\mathbf{Me}}$	−9.4	−14.9	−25.6	−24.0
$\mathbf{6}^{\mathbf{Me}}$	−3.0	−7.7	−4.9	−8.6

[a] For the short C2 linker, only the apical phosphine ligand is possible.

In general, complexes **3**, **5**, **6** prefer the apical ligand position due to steric reasons. In case of complex $\mathbf{4}^{\mathbf{Me}}$, however, the strain caused by the butyl tether is pronounced for the apical form and the basal isomer is energetically favoured. With the exception of complex $\mathbf{4}^{\mathbf{Me}}$, an increase in tethering chain length leads to an energetic preference of the apical over the basal rotamer (Table 2). Computational design of the tethering chain length thus allows to suggest suitable target complexes for the coordination preference of the phosphine ligand, and an estimate of the energy difference between the two isomers. Generally, BP86 and B3LYP underestimate the energy difference between the rotamers by 5–15 kJ mol^{-1}.

Rotational barriers. The energy barriers for the rotation of the $Fe(CO)_2PL_3$-subunit are obtained from calculations of the transition states of the transformation from the phosphine ligand in the apical into the basal position. In the literature, for the hexacarbonyl complex a 60° rotation of the three ligands is suggested,[20] whereby one of the carbonyl ligands moves to a semi-bridging position. This structure was used as a starting point and transition states were calculated for [FeFe](mcbdt)$(CO)_6$ **1**, for the reference complex $\mathbf{6}^{\mathbf{Me}}$ and for both the propyl- and butyl-tethered complexes $\mathbf{3}^{\mathbf{Me}}$ and $\mathbf{4}^{\mathbf{Me}}$. All structures were true transition states containing only one imaginary frequency in the vibrational frequency analysis. All structures were calculated at the DFT level with BP86, B3LYP, PWPB95 functionals and local coupled-cluster CCSD(T) as reference. Fig. 6 shows a representative rotational energy profile for the propyl-tethered complex **3**. The values for all complexes are given in Table 3.

The starting compound **1** and the functionalized reference compound **6** display almost identical barriers to rotation. This shows that the terminal phosphine does not affect the rotational energies of the barrier. Since the ethyl-tethered complex **2** only affords an apical structure, no rotation barrier can be reported.

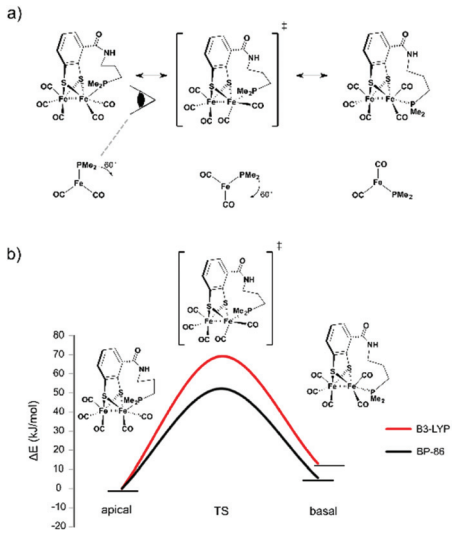

Fig. 6 (a) Anticipated rotation from apical *via* transition state to basal form. (b) Calculated rotational barrier for the propyl-tethered complex.

Table 3 Rotational barriers for the apical to basal conversion in kJ mol^{-1}

	BP86	B3LYP	PWPB95	DLPNO-CCSD(T)
1	41.4	54.5	32.2	57.1
$\mathbf{2^{Me}}$	n.a.			
$\mathbf{3^{Me}}$	52.2	69.1	44.9	72.8
$\mathbf{4^{Me}}$	23.5	37.4	21.9	45.4
$\mathbf{6^{Me}}$	40.4	55.7	35.0	60.4

The highest rotational energy barrier of all complexes was observed for propyl-tethered complex **3**. Compared to the reference complex **6**, an increase of the rotation barrier by 12–14 kJ mol^{-1} was calculated, depending on the level of calculation. This narrow range indicates the consistency of the *relative* energies although the absolute energies vary with the level of calculation. In contrast, complex **4** with a butyl tether did not show an increase in rotation energy barrier. The butyl tether allows too much structural flexibility and therefore the energy barrier is lower. As a matter of fact, it displays the lowest barrier of all complexes. For $\mathbf{4^{Me}}$, also the energy difference between basal and apical structures is lowest and only for this complex the basal rotamer is preferred. The butyl chain in the apical rotamer is highly strained, which disfavours this structure. Presumably, the rotation energy is decreased due to this fact.

Protonation studies. In order to validate our hypothesis that the tethering ligand in complex **3** would stabilize a terminal hydride, we treated complex **3** with $HBF_4{\cdot}Et_2O$. Unfortunately, we were not able to obtain any evidence for the protonated species, since the complex decomposed upon treatment. It seems that the mono-phosphine complex is not basic enough to be protonated directly at the iron center.[21d] Instead, we believe that the protonation occurs at the sulfur, leading to decomposition of the complex. We found for the propyl-tethered complex that formation of the bridging hydride is favored by 90 kJ mol^{-1} (BP86) and 131 kJ mol^{-1} (B3LYP) for the apical conformer. For the basal configuration, however, this energy difference reduces to 49 kJ mol^{-1} (BP86) and 76 kJ mol^{-1} (B3LYP) which shows that the approach to stabilize the basal configuration is at least partially successful and promising. The reason for this is the formation of a semi-bridging μ-CO complex when complex **3** is protonated at one of the iron atoms.

Conclusions

A new series of [FeFe]-hydrogenase model complexes with phosphine ligands that are covalently tethered to the bridging bdt ligand and coordinated to one iron centre has been prepared. The complexes have been characterized by FT-IR, ^{31}P-NMR spectroscopy and HR-MS. A detailed theoretical investigation was performed on the model complexes to study the effect of tethering ligands on the rotation of the terminal $Fe(CO)_2PL_3$-subunit. The highest energy barrier for the rotation has been found for the propyl-tethered complex **3** compared to the hexacarbonyl precursor **1** and the reference compound **6** that is lacking the linkage. The propyl-tethered complex **3** is thus the most promising candidate in the series presented for investigating protonation and the formation of a terminal hydride. The butyl-tethered complex **4** was the only complex with the phosphine in basal position being the lowest rotamer. All other complexes preferred the phosphine ligands in apical position although the energy differences are small. Restricting the rotation can potentially lead to the stabilization of the reactive terminal hydride, which is considered to be an important intermediate in the catalytic cycle of hydrogen evolution.

Experimental

Synthetic procedures

Fe_2(mcbdt)(CO)$_6$ (1). The synthesis was performed according to modified literature procedures.[21] 1,2-Benzenedithiol (500 mg, 3.5 mmol, 1 equiv.) was added to a schlenk flask under argon. The yellow solid was dissolved in dry hexane (20 ml) and TMEDA (0.53 ml, 3.54 mmol, 1.01 equiv.) was added, resulting in a yellowish-white precipitate. The mixture was cooled to −78 °C and ^{n}BuLi (2.5 M solution in hexane, 8.4 ml, 21 mmol, 6 equiv.) was added slowly. After stirring 30 min at −78 °C, the mixture was allowed to warm up to RT and then stirred for 2 h. The slightly yellow mixture was then again cooled to 0 °C and a stream of CO_2 gas that was dried with P_2O_5 in advance, was led into the reaction mixture over 2 h. Immediately, a yellow solid precipitated which intensified the color rapidly. The mixture was allowed to warm up to RT and was then acidified with HCl (4 M). The mixture was extracted with Et_2O and dried over Na_2SO_4. After evaporation, a yellow solid was obtained. This crude product was dissolved in dry THF without further purification and added to a schlenk

flask, which was previously filled with $Fe_3(CO)_{12}$ (2.12 g, 4.2 mmol, 1.2 equiv.) under argon. The dark green mixture was refluxed for 40 min, whereby the color changed to dark red. The mixture was then allowed to cool to RT and the solvent removed under reduced pressure. The crude product was purified by flash chromatography (Et_2O), hexane, acetic acid (3 : 3 : 0.2). The product was obtained as the second red band (the first one was the bdt-bridged complex).

Yield: 300 mg (18%).

IR_{CO} (CH_2Cl_2): 2084, 2035, 2009, 1996, 1980, 1691 cm^{-1}.

^1H NMR: 7.20 (dd, J = 7.4, 0.9, 1H, H_{ortho}), 7.06 (dd, J = 7.7, 0.8, 1H, H_{para}), 6.69 (dd, J = 7.6, 1H, H_{meta}).

Fe_2(propylamide-mabdt)$(CO)_6$. To a solution of Fe_2(mcbdt)$(CO)_6$ (500 mg, 1.078 mmol, 1 eq.) in DCM was added PyBop (673 mg, 1.293 mmol, 1.1 eq.) and NEt_3 (0.1 mL, catalytic). After stirring the mixture for 10 minutes, propylamine (96 μL, 1.185 mmol, 1.2 eq.) was added and the mixture was stirred for another 1 h at ambient temperature. The mixture was then poured into 50 mL cold water and extracted with DCM, dried over $MgSO_4$ and the solvent was removed under reduced pressure to yield the product in nice crystalline red powder (324 mg, 60%).

IR_{CO} (MeCN): 2079, 2044, 2005.

Fe_2(propylamide-mabdt)$(CO)_5(PPh_2Me)$ (6). The hexacarbonyl precursor (100 mg, 0.198 mmol, 1 eq.) was dissolved in acetonitrile and Me_3NO (23 mg, 0.208 mmol, 1.1 eq.) was added. After 10 minutes of stirring at ambient temperature, the phosphine ligand PPh_2Me (80 mg, 0.4 mmol, 1.1 eq.) was added dropwise and the reaction mixture stirred for 4 h until ligand exchange was complete as indicated by IR. After removing the solvent, the dark red solid was dissolved in Et_2O, extracted with water and the organic layers were dried over $MgSO_4$. The solution was concentrated under reduced pressure to 4 ml and the product was then purified by flash chromatography (DCM). The product eluted as a dark red band and after removing the solvent it was obtained as dark red powder (58 mg, 43%).

IR_{CO} (MeCN): 2052, 1993, 1938.

^{31}P-NMR: 38.94 ppm.

HR-MS: calculated for $C_{28}H_{24}Fe_2NO_6PS_2Na$ found 699.94 (product + Na), and for $C_{28}H_{24}Fe_2NO_6PS_2$ (product + H) calculated 677.96, found 677.96 (product + H).

Fe_2(propyl-tethered-mabdt-PPh_2)$(CO)_5$ (3). Fe_2(mcbdt)$(CO)_6$ (1 eq.) was dissolved in acetonitrile, followed by PyBop (1.1 eq.) and NEt_3 (0.1 mL, catalytic). After stirring the mixture for 10 minutes at ambient temperature, 3-(diphenylphosphino)-1-propylamine (1.2 eq.) was added and the mixture was stirred at ambient temperature for about 5 h until completion of the reaction was observed by IR spectroscopy. The solvent was then removed under reduced pressure and the residue extracted with DCM and washed with water. The crude product was then purified by flash chromatography (DCM).

IR_{CO} (MeCN): 2048, 1989, 1931.

^{31}P-NMR: 32.8 ppm.

HR-MS: calculated for $C_{27}H_{20}Fe_2NO_6PS_2$ 660.92, found 661.92.

Fe_2(butyl-tethered-mabdt-PPh_2)$(CO)_5$ (4). The complex was prepared in analogy to **3**.

IR_{CO} (MeCN): 2051, 1992, 1934.

^{31}P-NMR: 49.9 ppm.

4-(diphenylphosphaneyl)butan-1-amine synthesis. Diphenylphosphine (0.47 mL, 2.685 mmol, 1 eq.) was dissolved in THF (20 mL) and added dropwise to ^{n}BuLi (1.18 mL, 2.954 mmol, 1.1 eq.) at −50 °C. The reaction mixture was allowed to slowly warm up to RT. 4-Bromobutyronitrile (397.4 mg, 2.685 mmol, 1 eq.) dissolved in THF (20 mL), was added dropwise and then the reaction mixture was heated up to 40 °C and stirred for 18 h. The reaction was quenched with water at 0 °C and the organic layer was separated. The aqueous layer was extracted with Et_2O. The combined organic phases were dried over $MgSO_4$ and the solvent was removed under reduced pressure.

Computational methods

Turbomole 6.2 and 7.0 were used for GGA and hybrid DFT calculations (Ahlrichs, R. TURBOMOLE 6.2 and 7.0; Universität Karlsruhe: 2010/2015. See http://www.turbomole.com).[22] Additional calculations used Orca 4.0.[30]

Structural optimizations were performed at the BP86[23] and the hybrid B3LYP[24] functionals and structures were verified to be minima and transition states, respectively. The resolution of the identity (RI-J) approximation[25] was used for the GGA calculations. The Ahlrichs' def2-TZVP and def2-TZVPP basis sets[26] were used as indicated. Additional single point calculations with the larger basis set at the BP86/def2-TZVP optimized structures using the double-hybrid PWPB95[27] functional and the local coupled-cluster DLPNO-CCSD(T) method[28] method were performed in order to obtain more accurate relative energies. For the CC calculation, tight threshold values (TightPNO) settings were employed.[29]

All the structures presented are geometry optimized in gas-phase. IR frequencies were obtained by analytical evaluation of the second derivative of the DFT energy expression. The lack of negative eigenvalues for all structures shows they are true minima. Transition state structures were optimized until the analytical vibrational frequency calculation resulted in only one imaginary frequency which corresponded to the terminal ligand rotation.

Conflicts of interest

There are no conflicts to declare.

Acknowledgements

Financial support for this work was provided by the Swedish Research Council, the Knut & Alice Wallenberg Foundation, and the Swedish Energy Agency. MS is grateful to the Max Planck Society for the Advancement of Science (MPG) and the COST Action CM1305 'ECOSTBio' for financial

support. Financial support received from SERB-DST, India, under project no. (ECR/2016/000382 to SM) is gratefully acknowledged.

References

1 M. Frey, *ChemBioChem*, 2002, **3**, 153–160.
2 J. W. Peters, *Science*, 1998, **282**, 1853–1858.
3 (*a*) D. W. Mulder, M. W. Ratzloff, M. Bruschi, C. Greco, E. Koonce, J. W. Peters and P. W. King, *J. Am. Chem. Soc.*, 2014, **136**, 15394–15402; (*b*) M. Winkler, M. Senger, J. Duan, J. Esselborn, F. Wittkamp, E. Hofmann, U.-P. Apfel, S. T. Stripp and T. Happe, *Nat. Commun.*, 2017, **8**, 16115.
4 V. Pelmenschikov, J. A. Birrell, C. C. Pham, N. Mishra, H. Wang, C. Sommer, E. Reijerse, C. P. Richers, K. Tamasaku, Y. Yoda, T. B. Rauchfuss, W. Lubitz and S. P. Cramer, *J. Am. Chem. Soc.*, 2017, **139**, 16894–16902.
5 C. Liu, J. N. T. Peck, J. A. Wright, C. J. Pickett and M. B. Hall, *Eur. J. Inorg. Chem.*, 2011, **2011**, 1080–1093.
6 A. R. Finkelmann, M. T. Stiebritz and M. Reiher, *Chem. Sci.*, 2014, **5**, 215–221.
7 (*a*) L.-C. Song, J. Cheng, J. Yan, H.-T. Wang, X.-F. Liu and Q.-M. Hu, *Organometallics*, 2006, **25**, 1544–1547; (*b*) M. Razavet, S. C. Davies, D. L. Hughes and C. J. Pickett, *Chem. Commun.*, 2001, 847–848; (*c*) S. J. George, Z. Cui, M. Razavet and C. J. Pickett, *Chem. – Eur. J.*, 2002, **8**, 4037–4046.
8 (*a*) A. Orthaber, M. Karnahl, S. Tschierlei, D. Streich, M. Stein and S. Ott, *Dalton Trans.*, 2014, **43**, 4537–4549; (*b*) M. Beyler, S. Ezzaher, M. Karnahl, M.-P. Santoni, R. Lomoth and S. Ott, *Chem. Commun.*, 2011, **47**, 11662–11664.
9 S. Ezzaher, J.-F. Capon, F. Gloaguen, F. Y. Pétillon, P. Schollhammer, J. Talarmin, R. Pichon and N. Kervarec, *Inorg. Chem.*, 2007, **46**, 3426–3428.
10 F. I. Adam, G. Hogarth, S. E. Kabir and I. Richards, *C. R. Chim.*, 2008, **11**, 890–905.
11 B. E. Barton, G. Zampella, A. K. Justice, L. de Gioia, T. B. Rauchfuss and S. R. Wilson, *Dalton Trans.*, 2010, **39**, 3011–3019.
12 B. E. Barton and T. B. Rauchfuss, *Inorg. Chem.*, 2008, **47**, 2261–2263.
13 B. E. Barton, M. T. Olsen and T. B. Rauchfuss, *J. Am. Chem. Soc.*, 2008, **130**, 16834–16835.
14 M. E. Carroll, B. E. Barton, T. B. Rauchfuss and P. J. Carroll, *J. Am. Chem. Soc.*, 2012, **134**, 18843–18852.
15 R. Zaffaroni, T. B. Rauchfuss, D. L. Gray, L. de Gioia and G. Zampella, *J. Am. Chem. Soc.*, 2012, **134**, 19260–19269.
16 D. Morvan, J.-F. Capon, F. Gloaguen, A. Le Goff, M. Marchivie, F. Michaud, P. Schollhammer, J. Talarmin, J.-J. Yaouanc, R. Pichon and N. Kervarec, *Organometallics*, 2007, **26**, 2042–2052.
17 D. Morvan, J.-F. Capon, F. Gloaguen, F. Y. Pétillon, P. Schollhammer, J. Talarmin, J.-J. Yaouanc, F. Michaud and N. Kervarec, *J. Organomet. Chem.*, 2009, **694**, 2801–2807.
18 P. Knörzer, A. Silakov, C. E. Foster, F. A. Armstrong, W. Lubitz and T. Happe, *J. Biol. Chem.*, 2012, **287**, 1489–1499.
19 (*a*) D. Schilter, J. M. Camara, M. T. Huynh, S. Hammes-Schiffer and T. B. Rauchfuss, *Chem. Rev.*, 2016, **116**, 8693–8749; (*b*) C. Tard and C. J. Pickett, *Chem. Rev.*, 2009, **109**, 2245–2274.
20 A. K. Vannucci, S. Wang, G. S. Nichol, D. L. Lichtenberger, D. H. Evans and R. S. Glass, *Dalton Trans.*, 2010, **39**, 3050–3056.
21 (*a*) S. Pullen, H. Fei, A. Orthaber, S. M. Cohen and S. Ott, *J. Am. Chem. Soc.*, 2013, **135**, 16997–17003; (*b*) W. W. Seidel, F. E. Hahn and T. Lügger, *Inorg. Chem.*, 1998, **37**, 6587–6596; (*c*) D. Sellmann, T. Becker and F. Knoch, *Chem. Ber.*, 1996, **129**, 509–519; (*d*) L. Schwartz, P. S. Singh, L. Eriksson, R. Lomoth and S. Ott, *C. R. Chim.*, 2008, **11**, 875–889.
22 R. Ahlrichs, M. Bär, M. Häser, H. Horn and C. Kölmel, *Chem. Phys. Lett.*, 1989, **162**, 165–169.
23 (*a*) A. D. Becke, *Phys. Rev. A*, 1988, **38**, 3098–3100; (*b*) J. P. Perdew, *Phys. Rev. B: Condens. Matter Mater. Phys.*, 1986, **33**, 8822–8824.
24 (*a*) A. D. Becke, *J. Chem. Phys.*, 1993, **98**, 1372–1377; (*b*) C. Lee, W. Yang and R. G. Parr, *Phys. Rev. B: Condens. Matter Mater. Phys.*, 1988, **37**, 785–789.
25 K. Eichkorn, O. Treutler, H. Öhm, M. Häser and R. Ahlrichs, *Chem. Phys. Lett.*, 1995, **240**, 283–290.
26 A. Schäfer, C. Huber and R. Ahlrichs, *J. Chem. Phys.*, 1994, **100**, 5829–5835.
27 S. Grimme, *J. Chem. Phys.*, 2006, **124**, 34108.
28 (*a*) C. Riplinger, B. Sandhoefer, A. Hansen and F. Neese, *J. Chem. Phys.*, 2013, **139**, 134101; (*b*) C. Riplinger, P. Pinski, U. Becker, E. F. Valeev and F. Neese, *J. Chem. Phys.*, 2016, **144**, 24109.
29 F. Pavošević, P. Pinski, C. Riplinger, F. Neese and E. F. Valeev, *J. Chem. Phys.*, 2016, **144**, 144109.
30 F. Neese, *Wiley Interdiscip. Rev.: Comput. Mol. Sci.*, 2012, **2**, 73–78.